International Symposium
On Turbulence and Shear Flow
Phenomena (TSFP-9)
June 30 - July 3, 2015 *Melbourne, Australia*

INTERACTIONS OF TURBULENCE AND SCALARS IN SHEAR-DRIVEN PREMIXED TURBULENT FLAMES USING DNS

Haiou Wang
School of Mechanical and Manufacturing Engineering, The University of New South Wales, Sydney, NSW 2052, Australia
haiou.wang@unsw.edu.au

Evatt R. Hawkes
School of Mechanical and Manufacturing Engineering, The University of New South Wales, Sydney, NSW 2052, Australia
School of Photovoltaic and Renewable Energy Engineering, The University of New South Wales, Sydney, NSW 2052, Australia
evatt.hawkes@unsw.edu.au

Hemanth Kolla
Combustion Research Facility, Sandia National Laboratories, Livermore, CA 94551, USA
hnkolla@sandia.gov

Jacqueline H. Chen
Combustion Research Facility, Sandia National Laboratories, Livermore, CA 94551, USA
jhchen@sandia.gov

ABSTRACT

The DNS database of modelling lean H_2/air combustion in a temporally evolving premixed slot-jet configuration is employed to investigate turbulence-scalar interactions in turbulent reacting flows. In contrast to previous DNS studies of turbulent premixed flames, a mean shear exists in the flow and drives the generation of small-scale turbulence in the shear layer. The orientations of the flame normal and vorticity are examined. It is found that the flame normal preferentially aligns with the most compressive strain rate of the mean flow and the vorticity preferentially aligns with the most extensive mean strain rate. The former is consistent with the fact that the flame front has a tendency to align with the extensive strain rate, while the latter is related to vortex stretching in turbulent flows. The alignment characteristics of the flame normal, vorticity, and turbulent strain rate field conditioned on various progress variable iso-surfaces are investigated. Their influence on the scalar gradients and the vorticity production reflecting the turbulence-scalar interactions are examined quantitatively.

INTRODUCTION

Premixed turbulent combustion is commonly encountered in practical combustion devices such as gas turbines, and spark-ignition engines. An improved understanding of the interactions between turbulence and chemistry is of great importance for turbulent combustion modelling as well as design of clean and efficient combustion devices. In the present paper, turbulence-flame interactions are studied by analysing the coupled dynamics of the scalar gradient, strain rate and vorticity. The directional preference of the scalar gradients with respect to the strain rate is of substantial importance for modelling premixed turbulent combustion. Specifically, the so-called scalar-turbulence interaction signified by $-\rho N_c(n_i S_{ij} n_j)$ is a source term in the transport equation for the scalar dissipation rate of the progress variable N_c. In the expression signified by $-\rho N_c(n_i S_{ij} n_j)$, ρ is the density, D is the diffusivity, n_i is the flame normal component and S_{ij} is the strain rate tensor defined as $S_{ij} = 0.5(\partial u_i/\partial x_j + \partial u_j/\partial x_i)$. The strain rate S_{ij} can be characterised by the principal eigenvalues λ_1, λ_2, and λ_3 designated by the convention $\lambda_1 \geq \lambda_2 \geq \lambda_3$, which are determined from the characteristic equation. The corresponding eigenvectors are $\mathbf{e}_1$, $\mathbf{e}_2$ and $\mathbf{e}_3$, respectively. The flame normal $\mathbf{n}$ is defined in terms of the progress variable c:

$$\mathbf{n} = -\nabla c / \left|\nabla c\right| \tag{1}$$

and points towards the reactants. The term $n_i S_{ij} n_j$ is also known as the flame normal strain rate a_n. When $n_i S_{ij} n_j$ is negative, turbulence produces scalar gradients, and the flame normal is most likely to align with the most compressive strain rate. Detailed investigations of the alignments between the scalar gradient and the strain rate eigenvectors have been reported in various configurations (Kerr, 1985; Ruetsch and Maxey, 1991; Rogers and Moin, 1987; Nomura and Elghobashi, 1993; Swaminathan and

Grout, 2006; Hamlington et al. 2011). It is found that in both turbulent flows with a passive scalar and low Damköhler flames, the scalar gradient preferentially aligns with the most compressive strain rate, producing the scalar gradient. However, in high Damköhler flames, dilatation from the flame front would be prominent and the scalar gradient has a tendency to align with the most extensive strain rate (Chakraborty and Swaminathan, 2007).

In turbulent flows, velocity gradients provide rich information regarding the local behaviour of turbulence. Small structures are usually described in terms of strain rate and vorticity. The vorticity is written as:

$$\boldsymbol{\omega} = \nabla \times \mathbf{u} \tag{2}$$

In the balance equation for enstrophy (the squared vorticity magnitude ω^2), $\omega_i S_{ij} \omega_j$ is the production term, which is balanced by the viscous term.

The directional features of $\mathbf{n}$, $\boldsymbol{\omega}$, and $\mathbf{e}_i$ are important in turbulence-flame interactions as they explicitly influence the interaction terms described above. For example, the normal strain rate, $n_i S_{ij} n_j$, could also be written as:

$$n_i S_{ij} n_j = \lambda_1 (\mathbf{e}_1 \cdot \mathbf{n})^2 + \lambda_2 (\mathbf{e}_2 \cdot \mathbf{n})^2 + \lambda_3 (\mathbf{e}_3 \cdot \mathbf{n})^2 \tag{3}$$

In a similar way, the production term of ω^2, $\omega_i S_{ij} \omega_j$, could be expressed as:

$$\omega_i S_{ij} \omega_j = \omega^2 [\lambda_1 (\mathbf{e}_1 \cdot \hat{\boldsymbol{\omega}})^2 + \lambda_2 (\mathbf{e}_2 \cdot \hat{\boldsymbol{\omega}})^2 + \lambda_3 (\mathbf{e}_3 \cdot \hat{\boldsymbol{\omega}})^2] \tag{4}$$

where $\hat{\boldsymbol{\omega}}$ is the normalised vorticity vector denoted by $\hat{\boldsymbol{\omega}} = \boldsymbol{\omega}/|\boldsymbol{\omega}|$.

It should be noted that in previous DNS studies of the directional features in turbulent flames, a mean shear was absent. In practical applications of turbulent combustion, a mean shear is essential to drive energy cascade, associated with vortex stretching. However, there is little knowledge from DNS how flames respond to mean shear. A notable exception is the early work by Trouvé (1993), which examined flame surface density evolution in a simple shear flow and using one-step chemistry. As discussed by Trouvé, it can be expected that the mean shear drives production of turbulence, which can then interact more significantly with the flame. In the absence of this mean driving force, the heat release of the flame can largely nullify small-scale mixing within the flame structure.

The objective of the present study is to understand how the mean shear in the turbulent premixed flame influences the orientations of the flame normal and vorticity, and the alignment characteristics of $\mathbf{n}$, $\boldsymbol{\omega}$, and $\mathbf{e}_i$ conditioned on the flame front. To this end, the DNS database (Hawkes et al., 2012) of a temporally evolving slot-jet configuration with a mean shear that drives strong turbulent mixing within the flame structure is employed. The paper is organised as follows. Section 2 describes the features of the DNS database. Section 3 presents the details about the directional features of $\mathbf{n}$, $\boldsymbol{\omega}$, and $\mathbf{e}_i$. Summary of the findings is given in Section 4.

DNS DATABASE DESCRIPTION

The simulations are completely described by Hawkes et al. (2012), and a brief summary is provided here. The schematic of the computation domain is depicted in Figure 1, which characterises a temporally evolving premixed slot-jet flame interacting with a turbulent shear layer in a rectangular box. The boundary conditions are periodic in the streamwise x and spanwise z directions while non-reflecting in the transverse y direction.

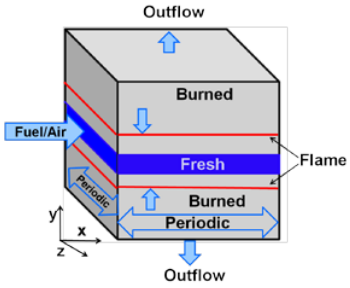

Figure 1. Configuration diagram of the DNS of H_2/air premixed turbulent combustion

Table 1. Initial parameters for DNS.

Re_j	Da_j	H (mm)	U (m/s)
10,000	0.13	2.7	312.6

The mean velocity field is initialised as a slab with width H and peak jet velocity U via a smooth tanh profile. A turbulence field with a velocity fluctuation of 4% of the main jet velocity is superimposed on the mean velocity profile. The scalar fields are initialised by performing one-dimensional precursor runs for two symmetric, flat laminar flames inwardly propagating in the y-direction, the species mass fractions and temperature of which are then copied throughout the x-z plane for three-dimensional runs.

The Reynolds and Damköhler numbers based on bulk jet parameters are given by $Re_{jet} = UH/\nu_0$, and $Da_j = t_j/\tau_L$ respectively, where ν_0 is the viscosity of the reactant, $t_j = H/U$ is the characteristic jet time and τ_L is the laminar flame time. Three cases (case Da-, case 0 and case Da+) are simulated by varying the peak jet velocity U and jet width H, such that Re_{jet} is held constant while Da_j varies (Hawkes et al. 2012). However, only the case with the smallest Damköhler number Da- is discussed in the present paper, as the results of the other two cases are quantitatively similar to those of case Da-. The main parameters of the DNS for case Da- are listed in Table 1.

The temperature of the reactant is 700 K, typical of gas turbine compressor exit temperatures. The equivalence ratio of the H_2/air mixture is 0.7, which is close to the neutral diffusive-thermal stability point. A 9 species and 21 elementary reactions mechanism for hydrogen oxidation is employed. The computations are among the largest single computations of any kind performed to date, involving 7 billion grid points each run and with each case running for 2-3 weeks on 120,000 processor cores.

Figure 2 shows the vorticity magnitude fields in a two-dimensional slice of 6H × 3H in a typical x-y plane at $t = 17.1t_j$. Note that $t = 17.1t_j$ is at the time of the maximum total flame surface area. Although the choice of the position of the slice is arbitrary, it is representative of

the flame. The flame position at the initial time is y = H + $15s_L t_j$ = 1.38H while at $17.1t_j$ the mean location is smaller than H. It is clear that as time progresses the shear-driven turbulence is able to develop and interacts with the flame. As a consequence, the flame front is increasingly distorted, reflected by the winkled iso-surfaces of the progress variable. There are more small-scale structures on the c = 0.1 iso-surface than on the c = 0.9 iso-surface, which is attributed to the difference of turbulence in the preheating and burning regions. As the equivalence ratio of the hydrogen-air mixture is 0.7, close to the neutral diffusive-thermal stability point, no preferential diffusion effect is observed in the present study. As shown in Figure 1, there are two planar flames propagating into a temporally developing plane jet of premixed reactant. Here, we only analyse the lower branch for the sake of brevity. However, the upper branch exhibites identical statistical features.

The vorticity magnitude is generally weaker in the product than in the reactant. The c = 0.5 iso-surface seperates intense vorticity regions from weak vorticity regions. This is because of the higher temperature in the product, where the kinematic viscosity increases significantly. To maintain a certain circulation, the size of each eddy increases as it crosses a reaction layer, which is depicted clearly in Figure 2. It is also seen that some strong eddies from the reactant would penetrate the flame and enter the reaction zone, thickening the flame. Thus, the vorticity in the turbulent flow would both wrinkle and thicken the flame. It should be noted that vorticity doesn't generate flame surface area directly. Instead, stretch (including strain and curvature effects) on the flame front is responsible for the increasing of the flame surface area.

Figure 3a shows the mean streamwise and transverse velocities across the flame brush. It is clear that both velocities increase approxiamately linearly with increasing y. Thus, the mean strain rate field does not vary when it crosses the flame brush. In order to understand the influence of the mean shear on the directional features in the flow, the total strain rate is split into two parts, i.e. the mean strain rate and the fluctuation strain rate: $S_{ij} = \overline{\boldsymbol{S}}_{ij} + s_{ij}$, where $\overline{\boldsymbol{S}}_{ij} = 0.5(\partial U_i/\partial x_j + \partial U_j/\partial x_i)$ and $s_{ij} = 0.5(\partial \boldsymbol{u}_i'/\partial x_j + \partial \boldsymbol{u}_j'/\partial x_i)$. The strain rate magnitude of the mean flow $(\overline{\boldsymbol{S}}_{ij}\overline{\boldsymbol{S}}_{ij})^{1/2}$ is 3.2×10^4 s^{-1}, while the average of the turbulent strain rate magnitude $(S_{ij}S_{ij})^{1/2}$ conditioned on the c = 0.5 iso-surface is about 3.0×10^5 s^{-1}, which is one order of magnitude higher than $(\overline{\boldsymbol{S}}_{ij}\overline{\boldsymbol{S}}_{ij})^{1/2}$. Thus, it is expected that the mean and fluctuation strain rates don't interact strongly and small-scale structures tend to be isotropic. The three eigenvectors of the mean strain rate tensor, $\bar{\mathbf{e}}_1$, $\bar{\mathbf{e}}_2$ and $\bar{\mathbf{e}}_3$, have been determined and are displayed in Figure 3b. The angle between the most extensive strain rate $\bar{\mathbf{e}}_1$ and the streamwise axis is 55.3°. Note that the strain rate component $\partial U_2/\partial y$ is positive as shown in Figure 3a, which is attributed to the heat release and dilation, so that the angle is larger than 45° in a pure shear flow, where all variables depend on y only and the only non-zero component of the velocity vector is U. The most compressive strain rate $\bar{\mathbf{e}}_3$ is perpendicular to $\bar{\mathbf{e}}_1$ in the x-y plane. The intermediate strain rate $\bar{\mathbf{e}}_2$ is along the spanwise axis (not shown). Also depicted in Figure 3b is a schematic of the position of the flame front. There is a preferential alignment between the flame front and the strain rate field, which will be discussed in more detail in the next section.

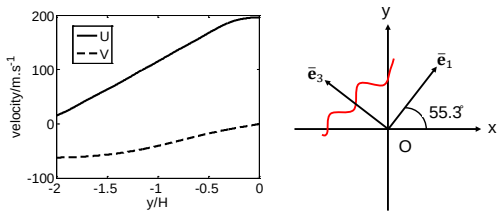

(a) (b)

Figure 3. (a) The mean streamwise and transverse velocities across the flame. (b) The strain rate eigenvectors of the mean flow.

RESULTS AND DISCUSSION

Figure 4 shows the probability density functions (PDFs) of α, the inclination angle of the flame normal in the streamwise-transverse (x-y) plane to the streamwise axis, and the PDFs of β, the polar angle between the flame normal and the spanwise axis. Here, α is defined as: α = arctan2(n_2, n_1), where quadrant-corrected arctan2 is the arctangent function with the two arguments n_2 and n_1. β is defined as: β = arccos(n_3). The sign convention for α and the coordinate system are depicted in Figure 5. Note that α varies from -180° to 180°, while β varies from 0 to 180°.

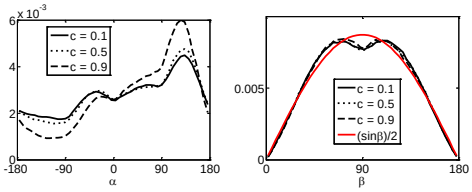

(a) (b)

Figure 4. PDFs of (a) α and (b) β.

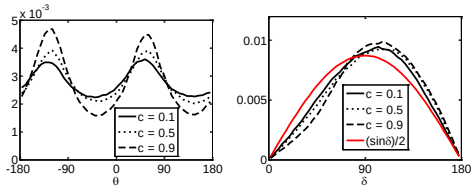

(a) (b)

Figure 6. PDFs of (a) θ and (b) δ.

It is clear that the most probable angle between the flame normal and the streamwise axis is about 135° on various progress variable iso-surfaces, and has a directional preference with the most compressive strain rate of the mean flow field (145.3° to the streamwise axis). This is consistent with the observation in Figure 2, where the direction of the most extensive strain rate is denoted by the black arrow. It is seen that the flame front has a tendency to align with the most extensive strain rate of the mean flow. A close inspection of Figure 4a reveals that on the c = 0.9 isosurface the most probable inclination angle is a little smaller than those on the other two iso-surfaces. This is because the c = 0.9 iso-surface is at the rear edge of the flame brush, where the change of the transverse velocity in the transverse direction, $\partial U_2/\partial y$, is smaller due to weaker reaction rate. Consequently, the strain rate tensor component $\partial U_1/\partial y$ dominates over $\partial U_2/\partial y$. Also it is shown that the directional preference of the flame normal with the most compressive strain rate of the mean flow field is stronger on the c = 0.9 iso-surface. This is due to the fact that the c = 0.9 iso-surface is less wrinkled at smaller scales than the other two iso-surfaces.

We proceed by studying the angle between flame normal and the spanwise axis, β. As the flame is statistically one-dimensional and the non-zero principal strain rates of the mean flow only exist in the x-y plane, it is expected that the distribution of β would be isotropic. Assuming an isotropic distribution of β indicates (Hawkes et al., 2009; Veynante et al., 2010): $P(\beta) = \sin(\beta)/2$. Figure 4b displays the distribution of β on various progress variable iso-surfaces. There is little difference of the distribution between different iso-surfaces. Moreover, the PDFs are very close to the isotropic distribution. Only some small discrepancies are observed near β = 90°.

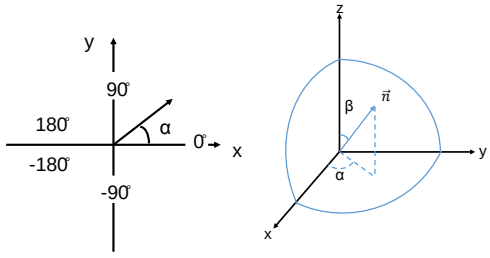

(a) (b)

Figure 5. Schematic of (a) α and (b) coordinate system

In a similar way, the orientation of the vorticity vector in terms of the inclination angle of the vorticity vector in the streamwise-transverse (x-y) plane to the streamwise axis, θ, and the polar angle between the vorticity vector and the spanwise axis, δ, could be analysed. Figure 6 shows the PDFs of δ and θ. The distribution of δ has two peaks. One is at θ = 55°, and the other one is at θ = -125°. As a matter of fact, the two angles indicate the same direction of the vortex axis as shown in Figure 5a.

Figure 6a illustrates the importance of vortex stretching by the mean shear to the dynamics of shear flows, i.e. the vorticity preferentially aligns with the most extensive strain rate of the mean flow (55.3° to the streamwise axis). Note that in an isotropic field without the mean shear, the vorticity would exhibit no directional preference. When the PDFs are weighted by the vorticity magnitude, this alignment characteristic would be more prominent (not shown), which implies that strong vortical structures are more likely to align with the most extensive strain rate of the mean flow.

The directional preference of the vorticity and the most extensive strain rate in the mean flow is also consistent with the results in non-reacting homogeneous shear flows by Rogers and Moin (1987) and Nomura and Elghobashi (1992). It is believed that vortex stretching plays an important role during this process (Tennekes and Lumley, 1973): vortices are more efficient to extract energy from the mean flow when their axes are aligned with the most extensive principal strain rate of the mean flow field.

The PDFs of δ on various progress variable iso-surfaces are displayed in Figure 6b. It is seen that the mean of δ is slightly larger than 90° and the PDFs are negatively skewed. The distribution of the angle δ is more isotropic on the c = 0.1 iso-surface than the other two iso-surfaces, as it is closer to the reactant, where the turbulent intensity is higher.

According to the above analyses, it is clear that the introduction of the mean shear plays an important role in the orientations of the flame normal and vorticity vectors in the turbulent flame. In particular, the flame normal preferentially aligns with the most compressive strain rate of the mean flow and the vorticity preferentially aligns with the most extensive strain rate. The former is consistent with the fact that the flame front has a tendency to align with extensive strain rates, while the latter is related to vortex stretching in turbulent flows.

In the following, we focus on the alignments between the vorticity, flame normal, and turbulent strain rate field. The importance of these alignments was emphasised in

Section 1. The orientation of the vorticity/flame normal relative to the principal strain-rate directions is determined by evaluating the absolute value of the cosine of the angle between the vorticity/flame normal vector and each of the strain rate eigenvectors at each grid point in the domain.

Firstly, the alignment between $\boldsymbol{\omega}$ and $\mathbf{e}_i$ is examined (Figure 7). In general the preferred alignment does not vary across the flame brush. It is clear that $\boldsymbol{\omega}$ preferentially aligns with the intermediate principal strain rate $\mathbf{e}_2$, preferentially misaligns with the most compressive principal strain rate $\mathbf{e}_3$, and weakly misaligns with the most extensive principal strain rate $\mathbf{e}_1$ on various progress variable iso-surfaces. The results are consistent with previous studies in non-reacting flows and premixed turbulent flames. She et al. (1991) suggested that the preferential alignment of $\boldsymbol{\omega}$ and the intermediate strain rate $\mathbf{e}_2$ was caused by the influence of the vorticity on the strain field. This point of view was consistent with Ashurst et al. (1987).

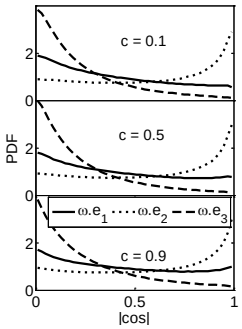

Figure 7. PDFs of $|\boldsymbol{\omega}\cdot\mathbf{e}_i|$

Figure 8 shows the PDFs of the alignment between $\mathbf{n}$ and $\mathbf{e}_i$. The flame normal preferentially aligns with the most compressive strain rate $\mathbf{e}_2$. The fluid dynamic strain dominates at this timing and the alignment characteristics are similar to those in non-reacting turbulent flows, which is consistent with prior studies for low Da number turbulent flames (Swaminathan and Grout, 2006; Chakraborty and Swaminathan, 2007; Hamlington et al. 2011). However, when we checked the results from case Da+, in which the Da number is four times larger than case Da-, the alignment between $\mathbf{n}$ and $\mathbf{e}_i$ was similar in both cases. Thus, it is suggested that a much larger Da number would be needed for the flame to reach a qualitatively different directional preference.

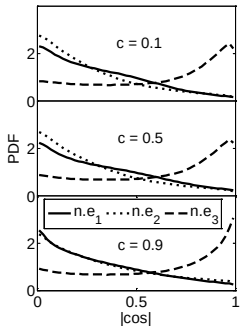

Figure 8. PDFs of $|\mathbf{n}\cdot\mathbf{e}_i|$

Figure 9 shows the PDFs of the normalised principal eigenvalues of the strain rate tensor. The eigenvalues are normalised by the laminar flame time scale. It is clear that the most probable value for the intermediate strain rate is zero, but its mean is positive. The possibility to have a positive λ_2 is much higher than a negative one (more than 80% of the samples have positive λ_2). It is also found that the distribution of λ_3 is broader and flatter than that of λ_1. It should be noted that the sum of the three principal strain rate eigenvalues is identical to the dilation ∇u, i.e. $\lambda_1+\lambda_2+\lambda_3=\nabla u$. In the present flame, the mean dilation conditioned on the flame front is positive due to the heat release, and the principal strain rate eigenvalues are dominated by two positive values and one negative value. A notable feature of the distributions is that the PDFs of the eigenvalues are broader on the c = 0.1 iso-surface. This is because turbulent straining is higher close to the reactant side.

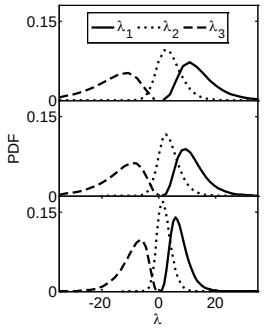

Figure 9. PDFs of the eigenvalues of the total strain rate tensor.

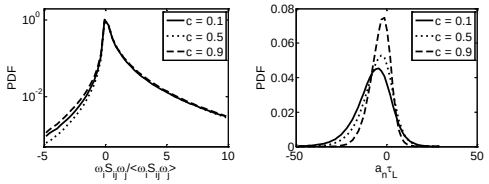

Figure 10. PDFs of $\omega_i S_{ij} \omega_j$ and a_n

It is interesting to know how the alignments influence the scalar gradients and the vorticity production in turbulent flames. As mentioned in Section 1, the production term of ω^2, $\omega_i S_{ij} \omega_j$, could be calculated in terms of the vorticity magnitude, strain rate eigenvalues, and alignments between $\boldsymbol{\omega}$ and $\mathbf{e}_i$. Figure 10 shows the PDFs of $\omega_i S_{ij} \omega_j$ normalised by its mean $\langle \omega_i S_{ij} \omega_j \rangle$. Here, $\langle \cdot \rangle$ denotes an ensemble average on the progress variable iso-surface. The figure is shown in a semi-logarithmic plot to emphasize the tails of the PDFs. Note that the production term is responsible for the creation of small-scale structure and the transfer of energy from large to small scales in turbulence. The distributions are positively skewed and close to each other in spite of some very small discrepancies which are found on the negative side. The term $\langle \omega_i S_{ij} \omega_j \rangle$ is positive and decreases as the progress variable increases. Positive $\omega_i S_{ij} \omega_j$ is expected because $\boldsymbol{\omega}$ preferentially aligns with the intermediate principal strain rate $\mathbf{e}_2$ as discussed earlier and λ_2 is most likely to be positive. However, it should be noted that it is also possible that $\boldsymbol{\omega}$ aligns with $\mathbf{e}_1$ or $\mathbf{e}_3$. To make this more quantitative, we computed the contributions of the three terms on the right hand side of Eq. (4) separately. On the c = 0.5 iso-surface, the three terms normalised by $\langle \omega_i S_{ij} \omega_j \rangle$ are 0.8, 0.5, and -0.3 respectively. This indicates that although $\boldsymbol{\omega}$ preferentially aligns with $\mathbf{e}_2$, the contribution from the most extensive strain rate dominates. This is because that $(\boldsymbol{\omega} \cdot \mathbf{e}_1)^2$ is weighted by λ_1, which is the largest eigenvalue of the strain rate tensor.

The distributions of $n_i S_{ij} n_j$, also known as the normal strain rate a_n, are studied as seen in Figure 10b. In contrast to $\omega_i S_{ij} \omega_j$, the PDFs are negatively skewed and have negative means. The negative normal strain rate would tend to bring the progress variable iso-surfaces toward each other, producing the scalar gradients. This is consistent with the fact that the flame normal has a directional preference with the most compressive strain rate. The distributions of a_n are further interpreted. On the right hand side of Eq. (3) the term $\lambda_3(\mathbf{n} \cdot \mathbf{e}_3)^2$ is dominant because of the preferential alignments between $\mathbf{n}$ and $\mathbf{e}_3$. As λ_3 is always negative, a_n is most likely to be negative. But $\lambda_3(\mathbf{n} \cdot \mathbf{e}_3)^2$ is not the only term that determines a_n. There are possibilities for a_n to be positive when the other two terms take effects. The three terms on the right hand side of Eq. (3) normalised by the laminar flame time scale are 2.2, 0.4, and -6.6 respectively on the c = 0.5 iso-surface.

CONCLUSION

In the present work, turbulence-scalar interactions in turbulent reacting flows are studied using the results from a temporally evolving premixed slot-jet configuration with a mean shear. Particular focus is placed on the orientations of the flame normal and vorticity and their alignment characteristics with the turbulent strain rate field. The flame normal has a preferred alignment with the most compressive strain rate of the mean flow while the vorticity preferentially aligns with the most extensive strain rate of the mean flow, which implies the importance of the mean shear to the turbulent topology and flame structure. It is also found that the vorticity preferentially aligns with the intermediate eigenvector of the turbulent strain rate. This is because of the influence of the vorticity on the strain field. The induced strain rate field aligns the weak extensive strain rate with the vorticity and the largest ones in the plane normal to the vortex axis. The effects of the alignments on the scalar gradients and the vorticity production in the flame are quantified.

ACKNOWLDGEMENTS

This work was supported by the Australian Research Council. The work at Sandia National Laboratories was supported by the Division of Chemical Sciences, Geosciences and Biosciences, the Office of Basic Energy Sciences, the US Department of Energy (DOE). This research used resources of Oak Ridge Leadership Computing Facility at Oak Ridge National Laboratory which is supported by the Office of Science of the DOE under contract No. DE-AC05-00OR22725. The research was also supported by computational resources on the Australian NCI National Facility through the National Computational Merit Allocation Scheme and Intersect partner shares.

REFERENCES

Ashurst, W. T., Kerstein, A. R., Kerr, R. M., and Gibson, C. H., 1987, "Alignment of vorticity and scalar gradient with strain rate in simulated Navier–Stokes turbulence", *Physics of Fluids (1958-1988)*, Vol 30, pp 2343-2353.

Chakraborty, N., and Swaminathan, N., 2007, "Influence of the Damköhler number on turbulence-scalar interaction in premixed flames. II. Model development", *Physics of Fluids*, Vol 19, 045104.

Hamlington, P. E., Poludnenko, A. Y., and Oran, E. S., 2011, "Interactions between turbulence and flames in premixed reacting flows", *Physics of Fluids*, Vol 23, 125111.

Hawkes, E. R., Chatakonda, O., Kolla, H., Kerstein, A. R., and Chen, J. H., 2012, "A petascale direct numerical simulation study of the modelling of flame wrinkling for large-eddy simulations in intense turbulence", *Combustion and Flame*, Vol 159, pp 2690-2703.

Hawkes, E. R., Sankaran, R., Chen, J. H., Kaiser, S. A., and Frank, J. H., 2009, "An analysis of lower-dimensional approximations to the scalar dissipation rate using direct numerical simulations of plane jet flames", *Proceedings of the Combustion Institute*, Vol 32, pp 1455-1463.

Kerr, R. M., 1985, "Higher-order derivative correlations and the alignment of small-scale structures in isotropic numerical turbulence", *Journal of Fluid Mechanics*, Vol. 153, pp. 31-58.

Nomura, K. K., and Elghobashi, S. E., 1993, "The structure of inhomogeneous turbulence in variable density nonpremixed flames", *Theoretical and Computational Fluid Dynamics*, Vol 5, pp 153-175.

Ruetsch, G. R., and Maxey, M. R., 1991, “Small-scale features of vorticity and passive scalar fields in homogeneous isotropic turbulence”, *Physics of Fluids A: Fluid Dynamics*, Vol. 3, pp 1587-1597.

Rogers, M. M., and Moin, P., 1987, “The structure of the vorticity field in homogeneous turbulent flows”, *Journal of Fluid Mechanics*, Vol 176, pp 33-66.

She, Z. S., Jackson, E., and Orszag, S. A., 1991, “Structure and dynamics of homogeneous turbulence: models and simulations. Proceedings of the Royal Society of London”, *Series A: Mathematical and Physical Sciences*, Vol 434, pp 101-124.

Swaminathan, N., and Grout, R. W., 2006, “Interaction of turbulence and scalar fields in premixed flames”, *Physics of Fluids*, Vol 18, 045102.

Tennekes, H., and Lumley, J. L., 1972, “A first course in turbulence”, MIT press.

Trouvé, A., 1994, “The production of premixed flame surface area in turbulent shear flow”, *Combustion and flame*, Vol 99, pp 687-696.

Veynante, D., Lodato, G., Domingo, P., Vervisch, L., and Hawkes, E. R., 2010, “Estimation of three-dimensional flame surface densities from planar images in turbulent premixed combustion”, *Experiments in Fluids*, Vol 49, pp 267-278.